A Continuously Tunable Bandpass Filter Using Distilled Water Based on Multiple-Mode Resonator

Jian-Hui Guo, Sai-Wai Wong, *Senior Member, IEEE*, Jing-Yu Lin, Yin Li, Long Zhang, *Member, IEEE*, Lei Zhu, *Fellow, IEEE*, Ze-Ming Xie, and Yejun He, *Senior Member, IEEE*

***Abstract*— In this letter, a continuously tunable bandpass filter (BPF) with low insertion loss using distilled water based on the stripline triple-mode resonator (TMR) is first presented. The configurability of proposed BPF is achieved by using six polytetrafluoroethylene (PTFE) tubes located above the surface of the TMR circuit. These tubes are filled with distilled water. By adjusting the amount of distilled water inside these tubes, the equivalent electrical length of the transmission line changes, which can change the resonant frequency of the TMR. It is demonstrated in simulated and measured results that the center frequency tuning of the proposed BPF is ranged from 1.06 to 1.29 GHz with a fractional bandwidth (FBW) of 16.5%–19.2% and the measured insertion loss is varied within 1–0.4 dB. The measured results are highly consistent with the simulated results.**

***Index Terms*— Distilled water, low insertion loss, triple-mode resonator (TMR), tunable bandpass filter (BPF).**

I. Introduction

In WIRELESS communication systems, high data rate, large capability, wide frequency range, and the supporting of multiple frequencies are the trend of radio frequency front-end circuit development. In order to meet the requirement of the wide frequency range and the multiple frequency range, a tunable bandpass filter (BPF) is a good candidate. There are many techniques that can be used to design tunable BPF, including microelectromechanical systems (MEMS) [1], [2], varactor-loaded [3]–[5] and so on. Tunable BPFs designed using MEMS technique have the advantages of small size and easy integration, but they have some limitations, e.g., higher cost. Tunable BPF designed based on varactor-loaded technique is relatively cheaper, but it has a limited power capacity and a higher insertion loss. In order to overcome these disadvantages, some tunable BPFs designed based on the microfluidic technique have emerged. These microfluidic BPFs, such as distilled water, have higher power capacity and lower insertion loss. In [6], a fourth-order tunable BPF based on an inverted microstrip is presented. Some polytetrafluoroethylene (PTFE) tubes filled with/without deionized water are placed between the microstrip lines and ground to achieve a frequency reconfigurability. In [7], a novel tunable differential BPF based on a dual-mode patch resonator is presented. The frequency reconfigurability is achieved by placing some tubes filled with/without distilled water between the patch and ground. Moreover, the center frequency of the BPF can be precisely controlled by selecting different water-filling sequences. In [8], a novel microfluidically tunable BPF is presented. It contains two quarter-wavelength short-circuited resonators and some plastic tubes placed above the resonators. Different frequency tuning states are obtained by selecting different water-filling sequences and locations of the plastic tubes. However, most of the reported tunable BPFs using distilled water are not continuously tunable.

In this letter, a novel continuously tunable BPF using distilled water based on a triple-mode resonator (TMR) [9]–[11] is first proposed. This proposed tunable BPF has achieved the widest tuning range and a competitive in-band insertion loss.

II. Geometry, Analysis, and Design

Fig. 1 shows the geometrical structure of the proposed tunable BPF. The proposed filter consists of three layers of substrate and three layers of metal as shown in Fig. 1(a). Substrate 1 and Substrate 3 are RO4350B with a thickness of 1.524 mm, and Substrate 2 is RO4350B with a thickness of 0.254 mm. The length and width of each substrate are l and w, respectively. The TMR is located on Substrate 2. The marked dimension of TMR of Metal 2 is shown in Fig. 1(b).

Manuscript received October 23, 2019; revised December 22, 2019 and February 22, 2020; accepted March 18, 2020. Date of publication April 9, 2020; date of current version May 8, 2020. This work was supported in part by the Shenzhen Science and Technology Programs under Grant JCYJ20180305124543176 and Grant JCYJ20190728151457763, in part by the Natural Science Foundation of Guangdong Province under Grant 2018A030313481, in part by the Shenzhen University Research Startup Project of New Staff under Grant 860-000002110311 and Grant 20188082, and in part by the National Natural Science Foundation of China under Grant 81771955. *(Corresponding author: Sai-Wai Wong.)*

Jian-Hui Guo is with the College of Electronic and Information Engineering, Shenzhen University, Shenzhen 518060, China, and also with the School of Electronic and Information Engineering, South China University of Technology, Guangzhou 510640, China.

Sai-Wai Wong, Yin Li, Long Zhang, and Yejun He are with the College of Electronic and Information Engineering, Shenzhen University, Shenzhen 518060, China (e-mail: wongsaiwai@ieee.org).

Jing-Yu Lin is with the School of Electrical and Data Engineering, University of Technology Sydney, Ultimo, NSW 2007, Australia.

Lei Zhu is with the Department of Electrical and Computer Engineering, Faculty of Science and Technology, University of Macau, Macau 999078, China.

Ze-Ming Xie is with the School of Electronic and Information Engineering, South China University of Technology, Guangzhou 510640, China.

Color versions of one or more of the figures in this letter are available online at http://ieeexplore.ieee.org.

Digital Object Identifier 10.1109/LMWC.2020.2982806

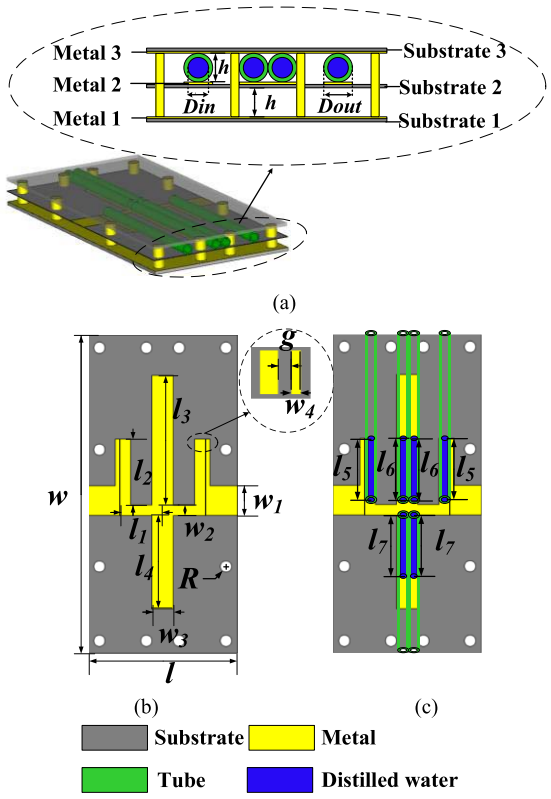

Fig. 1. Geometrical structure of proposed tunable BPF. (a) 3-D view. (b) Top view of the circuit layout. (c) Position of water tubes.

Metal 1 and Metal 3 are used for grounding purpose. Some metal posts of radius R are used to sustain each substrate layer, reduce radiation loss, and reduce surface wave. Six PTFE tubes with a dielectric constant of 2.1 filled with distilled water (permittivity $\varepsilon_{rw} = 78$, loss tangent 0.13) are placed between Metal 2 and Metal 3. In particular, two parallel tubes are installed along the surface of the two stubs, respectively. As shown in Fig. 1(c), some key parameters are marked. D_{out} and D_{in} represent the outer and inner diameters of water tubes, respectively, and h represents the height of the two air gaps for inserting PTFE tubes. The TMR contains a half wavelength open-circuited resonator with two open-circuited stubs. The length and width of the half-wavelength open-circuited resonator are $2^*(l_1 + l_2)$ and w_2, respectively. The length and width of the upper stub are l_3 and w_3, respectively, whereas the length and width of the lower stub are l_4 and w_3, respectively. The energy coupling between the input–output feedline and the resonator is achieved by a gap of distance g. L_5, l_6, and l_7 represent the water level filled inside the water tubes as shown in Fig. 1(c).

Fig. 2(a) shows the equivalent circuit of the TMR. Since the structure of this resonator is symmetrical. Thus, it can be analyzed by using the even- and odd-mode model. Fig. 2(b) shows the even mode and the odd mode equivalent circuits. Z_1, Z_2, θ_1, θ_2, and θ_3 refer to the characteristic impedance and electrical length of the transmission line, respectively. l_1, l_2, l_3, and l_4 refer to the physical length of transmission lines of TMR as shown in Fig. 1(b). In order to make the design simpler, Z_1 is equal to twice of Z_2. According to the even–odd mode analysis, the resonant condition for odd mode is $Y_{\text{in-odd}} = 0$,

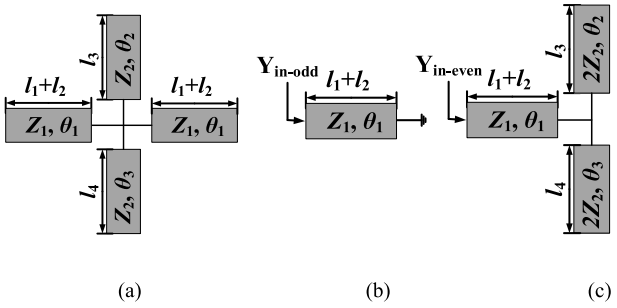

Fig. 2. (a) Equivalent circuit of the TMR. (b) Odd mode. (c) Even mode.

and the resonant condition for even mode is $Y_{\text{in-even}} = 0$. The three resonant frequencies can be derived as follows:

$$f_{\text{odd}} = \frac{c}{4(l_1 + l_2)\sqrt{\varepsilon_r}} \tag{1}$$

$$f_{\text{even1}} = \frac{c}{2(l_1 + l_2 + l_3)\sqrt{\varepsilon_r}} \tag{2}$$

$$f_{\text{even2}} = \frac{c}{2(l_1 + l_2 + l_4)\sqrt{\varepsilon_r}} \tag{3}$$

where f_{odd} means the resonant frequency of odd mode and f_{even1}, f_{even2} mean the resonant frequencies of the two even modes. c is the speed of light in the free space and ε_r is the effective dielectric constant. It can be seen from (1) to (3) that the values of l_1 and l_2 influence the three resonant frequencies, and the values of l_3 and l_4 control the f_{even1} and f_{even2}, independently. In order to form a good passband, the resonant frequency of the odd mode is between two even-mode resonant frequencies. Since the electric field distributions of three modes are different, the influence of the distilled water above different transmission lines is different. When the amount of water in the tube above the transmission line changes, the equivalent electrical length of the transmission line also changes accordingly as explained in [6]; thus, the three resonant frequencies change. Therefore, the operating frequency of the BPF can be tuned by adjusting the amount of distilled water in different tubes. Particularly, the amount of water injection is arbitrary and continuous; thus, the filter tuning is a continuous tuning process.

III. Simulated and Measured Results

Based on the above theoretical analysis, the proposed tunable BPF is designed by using an electromagnetic simulation software CST. The outer and inner diameters of the tube are 5 and 4 mm, respectively. Those optimized parameters are given: $w = 150$, $l = 70$, $w_1 = 14$, $w_2 = 5$, $w_3 = 10$, $w_4 = 2$, $l_1 = 20$, $l_2 = 31$, $l_3 = 61$, $l_4 = 44$, $g = 0.2$, $R = 1.5$, $H = 5$ (all in mm). Fig. 3 shows the variation of the absolute bandwidth of the BPF. In Fig. 3, as the value of water level l_7 increases, the cutoff frequency at upper band decreases, whereas as the value of water level l_6 increases, the cutoff frequency at lower band decreases. Thus, the fractional bandwidth (FBW) of the proposed BPF can be continuously controlled in the process of changing the water level l_6 and l_7. The initial state of the proposed BPF is designed without distilled water in water tubes. Fig. 4 shows the simulated and measured results. Fig. 5 shows the wideband simulated results. Obviously, as the amount of the

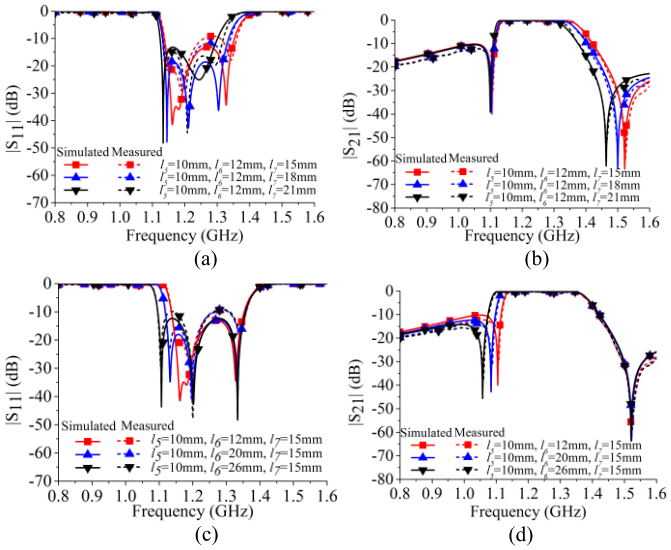

Fig. 3. Variation of the absolute bandwidth. (a) Variation of $|S_{11}|$ at the upper sideband. (b) Variation of $|S_{21}|$ at the upper sideband. (c) Variation of $|S_{11}|$ at the lower sideband. (d) Variation of $|S_{21}|$ at the lower sideband.

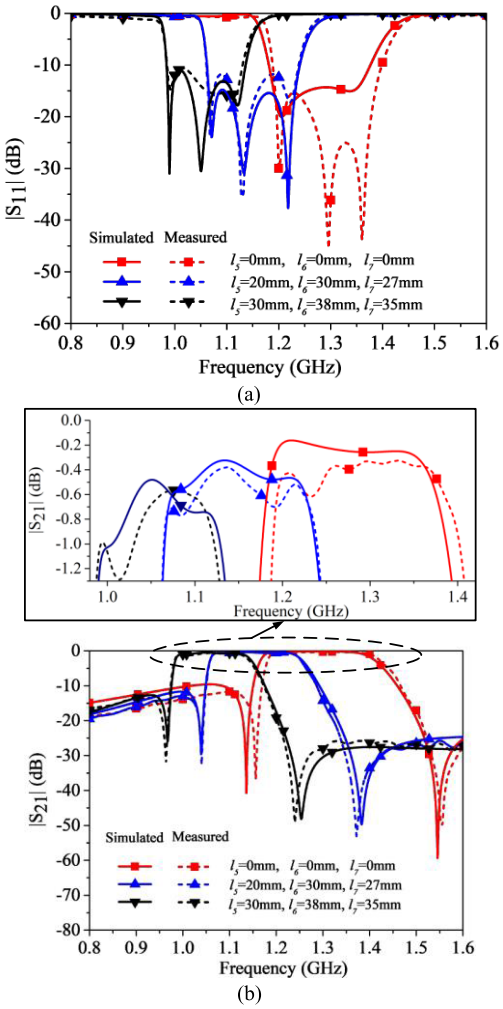

Fig. 4. Simulated and measured results. (a) $|S_{11}|$. (b) $|S_{21}|$.

distilled water in different tubes change, the center frequency of the BPF is tuned from 1.06 to 1.29 GHz with a FBW of 16.5%–19.2%. The measured insertion loss at center frequency

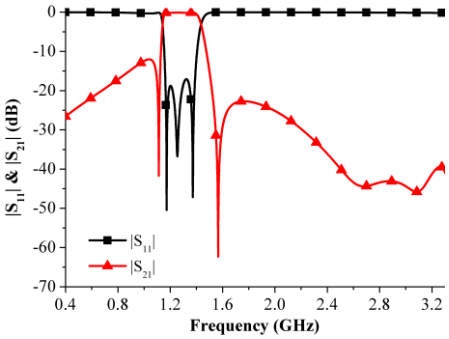

Fig. 5. Wideband simulated results ($l_5 = 0$ mm, $l_6 = 0$ mm, $l_7 = 0$ mm).

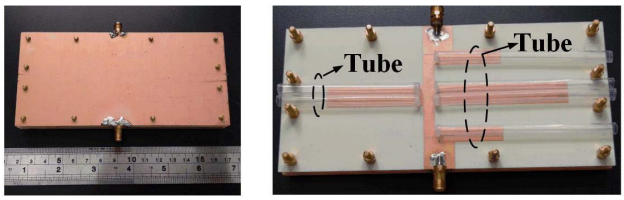

Fig. 6. Photograph of the fabricated BPF.

TABLE I
COMPARISON WITH OTHER TUNABLE BPFS USING DISTILLED WATER

Ref.	Order	IL (dB)	TR (%)	FBW (%)	Tuning Type	Size (λ_g^2)
[6]	4	<0.6	19	37.5-40	Discretely	1.88
[7]	2	0.78-1.18	9	15.5-16.1	Discretely	0.48
[8]	2	<1	5	NA	Discretely	0.12
This Work	**3**	**0.4-1**	**22**	**16.5-19.2**	**Continuously**	**0.45**

Ref.: Reference; IL: Insertion Loss; TR: Frequency Tuning Range; FBW: Fractional Bandwidth; λ_g: Guided-wavelength at the Lowest Frequency.

is changed from 1 to 0.4 dB with the measured return loss below 10 dB. It is noteworthy that the loss of water only affects slightly. Under the same conditions, if the loss of water is not considered, the simulated insertion loss at center frequency is reduced by at most 0.3 dB. Finally, the fabricated BPF is shown in Fig. 6. In practical application, the water tube can be connected to an electrical controlled water pump. For precise control of frequency tuning, the amount of water injection can be calibrated with the frequency variation. Table I shows the comparison with other recently reported tunable BPFs using distilled water. The tuning range of proposed tunable BPF is the widest among those reported works. Moreover, the insertion loss of proposed BPF is very competitive among those reported tunable BPFs using distilled water.

IV. CONCLUSION

In this letter, a continuously tunable BPF with low insertion loss using distilled water based on the stripline TMR has been first presented. Our proposed BPF has achieved the widest tuning range and a competitive in-band insertion loss. The center frequency of the BPF can be tuned from 1.06 to 1.29 GHz with a variation in FBW of 16.5%–19.2%. The measured insertion loss at center frequency has been varied from 1 to 0.4 dB during the tuning process. A good agreement has been obtained between the simulated and measured results.

REFERENCES

[1] K. Entesari and G. M. Rebeiz, "A 12-18-GHz three-pole RF MEMS tunable filter," *IEEE Trans. Microw. Theory Techn.*, vol. 53, no. 8, pp. 2566–2571, Aug. 2005.

[2] N. Kumar and Y. K. Singh, "RF-MEMS-based bandpass-to-bandstop switchable single- and dual-band filters with variable FBW and reconfigurable selectivity," *IEEE Trans. Microw. Theory Techn.*, vol. 65, no. 10, pp. 3824–3837, Oct. 2017.

[3] H. Guo, J. Ni, and J. Hong, "Varactor-tuned dual-mode bandpass filter with nonuniform Q distribution," *IEEE Microw. Wireless Compon. Lett.*, vol. 28, no. 11, pp. 1002–1004, Nov. 2018.

[4] X. T. Zou, Z. J. Yang, F. Wei, B. Li, and X. W. Shi, "Compact balanced single-band and dual-band BPFs with controllable bandwidth using foldeds-shaped slotline resonators (FSSRs)," *FREQUENZ*, vol. 73, nos. 1–2, pp. 13–18, Jan. 2019.

[5] Z. J. Yang, G. X. Xiao, F. Wei, B. Zhou, and B. Li, "A balanced dual-band bandpass filter with independently tunable differential-mode frequencies," *Int. J. RF Microw. Comput.-Aided Eng.*, vol. 28, no. 6, 2018, Art. no. e21295.

[6] D. L. Diedhiou, R. Sauleau, and A. V. Boriskin, "Microfluidically tunable microstrip filters," *IEEE Trans. Microw. Theory Techn.*, vol. 63, no. 7, pp. 2245–2252, Jul. 2015.

[7] W.-J. Zhou, H. Tang, and J.-X. Chen, "Novel microfluidically tunable differential dual-mode patch filter," *IEEE Microw. Wireless Compon. Lett.*, vol. 27, no. 5, pp. 461–463, May 2017.

[8] W.-J. Zhou and J.-X. Chen, "Novel microfluidically tunable bandpass filter with precisely-controlled passband frequency," *Electron. Lett.*, vol. 52, no. 14, pp. 1235–1236, Jul. 2016.

[9] X. Guan, S. Jiang, P. Chen, L. Shen, D. Huang, and H. Liu, "An ultra-wideband bandpass filter using cross-shaped triple-mode resonator," in *Proc. Int. Conf. Microw. Millim. Wave Technol.*, May 2010, pp. 559–561.

[10] J.-S. Hsieh and C.-M. Tsai, "Synthesis of filters with stub-loaded multiple-mode resonators," *IEEE Microw. Wireless Compon. Lett.*, vol. 21, no. 10, pp. 516–518, Oct. 2011.

[11] S. Sun and L. Zhu, "Multiple-resonator-based bandpass filters," *IEEE Microw. Mag.*, vol. 10, no. 2, pp. 88–98, Apr. 2009.